

Fast rotating Blue Stragglers in the globular cluster M4¹

L. Lovisi², A. Mucciarelli², F.R. Ferraro², S. Lucatello^{3,4}, B. Lanzoni², E. Dalessandro², G. Beccari⁵, R.T. Rood⁶, A. Sills⁷, F. Fusi Pecci⁸, R. Gratton³, G. Piotto⁹

² *Dipartimento di Astronomia, Università degli Studi di Bologna, via Ranzani 1, I-40127 Bologna, Italy*

³ *INAF- Osservatorio Astronomico di Padova, Vicolo dell'Osservatorio 5, I-35122 Padova, Italy*

⁴ *Excellence Cluster Universe, Technische Universität München, Boltzmannstr. 2, D-85748, Garching, Germany*

⁵ *ESA, Space Science Department, Keplerlaan 1, 2200 AG Noordwijk, Netherlands*

⁶ *Astronomy Department, University of Virginia, P.O. Box 400325, Charlottesville, VA, 22904, USA*

⁷ *Department of Physics and Astronomy, McMaster University, 1280 Main Street West, Hamilton, ON, L8S 4M1, Canada*

⁸ *INAF- Osservatorio Astronomico di Bologna, Via Ranzani, 1, 40127 Bologna, Italy*

⁹ *Dipartimento di Astronomia, Università di Padova, Vicolo dell'Osservatorio 5, I-35122 Padova, Italy*

1 July, 10

ABSTRACT

We have used high resolution spectra obtained with the spectrograph FLAMES at the ESO Very Large Telescope to determine the kinematical properties and the abundance patterns of 20 blue straggler stars (BSSs) in the globular cluster M4. We found that $\sim 40\%$ of the measured BSSs are fast rotators (with rotational velocities $> 50 \text{ km s}^{-1}$). This is the largest frequency of rapidly rotating BSSs ever detected in a globular cluster. In addition, at odds with what has been found in 47 Tucanae, no evidence of carbon and/or oxygen depletion has been revealed in the sample of 11 BSSs for which we were able to measure the abundances. This could be due either to low statistics, or to a different BSS formation process acting in M4.

Subject headings: blue stragglers; globular clusters: individual (NGC 6121); stars: abundances; stars: evolution; techniques: spectroscopic

1. Introduction

Blue straggler stars (BSSs) are brighter and bluer (hotter) than the main sequence (MS) turnoff and they mimic a rejuvenated stellar population in globular clusters (GCs). From their position in the colour-magnitude diagram (CMD) and from direct measurements (Shara et al. 1997; see also Ferraro, Fusi Pecci & Bellazzini 1995), they are known to be more massive than the normal MS stars, thus indicating that some process able to increase the initial mass of single stars must be at work: BSSs could be generated by collision-induced stellar mergers (COL-BSSs; Hills & Day 1976), or they may form by the mass-transfer activity in a binary system (MT-BSSs; McCrea 1964), possibly up to the complete coalescence of the two companions. BSSs in different environments could have different origins (Fusi Pecci et al. 1992). In particular, BSSs in loose GCs might be produced from the coalescence of primordial binaries, whereas in high-density GCs BSSs might arise mostly from stellar collisions, particularly those involving binaries. Moreover, there is evidence that both mechanisms could act simultaneously within the same cluster (see the two distinct sequences of BSSs recently discovered in M30 by Ferraro et al. 2009), also depending on the different stellar densities at various distances from the cluster center. This is suggested by the bimodality of the BSS radial distribution detected in several GCs (Ferraro & Lanzoni 2009 for a review). While theoretical predictions about the properties of BSSs generated by different formation channels are still uncertain and controversial, the search for chemical patterns onto the BSS surface seems to be the most promising route to discriminate between the two scenarios. In fact, hydrodynamic simulations (Lombardi et al. 1995; Sarna & DeGreve 1996) suggest that very little mixing should occur between the inner cores and the outer envelopes of the colliding stars (hence COL-BSSs should not show any abundance anomaly), while depleted surface abundances of carbon (C) and oxygen (O) are expected for MT-BSSs, since the accreted material should come from the core region of a peeled parent star where nuclear processing has occurred. Indeed this seems to be the case for the sub-

¹Based on observations collected at the ESO-VLT under program 081.D-0356. Also based on observations collected at the ESO-MPI Telescope under program 69.D-0582, and with the NASA/ESA *HST*, obtained at the Space Telescope Science Institute, which is operated by AURA, Inc., under NASA contract NAS5-26555.

sample of BSSs with significant CO-depletion discovered in 47 Tucanae (47Tuc) by Ferraro et al. (2006, hereafter F06).

In this framework, we are conducting an extensive survey of surface abundance patterns and kinematical properties of BSSs in a selected sample of GCs, by using the Very Large Telescope (VLT) of the European Southern Observatory (ESO). In this letter we report on new findings of this project concerning the GC M4.

2. Observations

The observations were performed at the ESO-VLT during three nights in June 2008, using the multi-object facility FLAMES-GIRAFFE (Pasquini et al. 2002). The sample includes 20 BSSs, 53 subgiant branch stars (SGBs) and 38 red giant branch stars (RGBs). The spectroscopic target selection has been performed on a photometric catalog obtained by combining ACS@HST data for the central region (i.e., at radial distances $r < 100''$) and WFI@ESO observations for the outer region. We have also taken into account the stellar proper motions for the wide-field sample (Anderson et al. 2006), and discarded all the stars having a source with a comparable or a brighter luminosity at a distance smaller than $3''$. The selected BSS sample represents $\sim 70\%$ of the entire population within $800''$ (≈ 11 core radii) from the cluster centre (Lanzoni et al. 2010, in preparation), with $\sim 50\%$ of them being located at $r < 100''$. The RGBs and SGBs have been selected from the WFI sample at $100'' < r < 800''$.

Three different setups were used for the spectroscopic observations: HR15, HR18 and HR22, suitable to sample the $H\alpha$ line, the OI triplet at $\lambda \simeq 7774 \text{ \AA}$, and the CI line at $\lambda \simeq 9111 \text{ \AA}$, respectively. Exposure times amount to one hour for the HR15 setup, and two hours each for the HR18 and HR22. Spectra have been pre-reduced using the standard GIRAFFE ESO pipeline. The accuracy of the wavelength calibration has been checked by measuring the position of a number of emission telluric lines (Osterbrock et al. 1996). Then, we subtracted the mean sky spectrum from each stellar spectrum. By combining the exposures, we finally obtained median spectra with signal-to-noise ratios $S/N \simeq 50 - 100$ for the selected BSSs and SGBs, and $S/N \simeq 100 - 300$ for the RGBs.

3. Analysis and results

The procedure adopted to derive the radial and rotational velocities, and the [O/Fe], [C/Fe] and [Fe/H] abundance ratios for the observed sample is summarized below. Table 1

lists the values obtained for the BSSs, together with the adopted temperatures and gravities.

Radial velocities – Radial velocities (V_{rad}) were measured using the IRAF task *fxcor* that performs the Fourier cross-correlation between the target spectra and a template of known radial shift, following the prescriptions by Tonry & Davis (1979). As a template for the samples of BSSs, SGBs and RGBs we used the corresponding spectra with the highest S/N ratio, for which we computed V_{rad} by measuring the wavelength position of a few tens of metallic lines. Radial velocity values obtained from the three different setups are consistent each other within the uncertainties which are of the order of 0.5 km s^{-1} for the SGB stars and most of the BSSs (see Table 1), and 0.15 km s^{-1} for the RGBs. For the fast rotating stars (see below) V_{rad} has been estimated from the centroid of the $\text{H}\alpha$ line, which is almost unaffected by rotation.

Figure 1 shows the derived V_{rad} distribution for the giants (RGBs+SGBs) and the BSSs. The mean radial velocity of the total sample is $\langle V_{\text{rad}} \rangle = 71.28 \pm 0.50 \text{ km s}^{-1}$, with a dispersion $\sigma = 5.26 \text{ km s}^{-1}$. The distribution for the giant stars is peaked at nearly the same value, $\langle V_{\text{rad}} \rangle = 71.25 \pm 0.43$ ($\sigma = 4.08$) km s^{-1} , which we adopt as the systemic velocity of M4. This is in good agreement with previous determinations (Peterson et al. 1995, Harris 1996, Marino et al. 2008, Sommariva et al. 2009, Lane et al. 2009). The average of the BSS radial velocity distribution is also similar, $\langle V_{\text{rad}} \rangle = 71.40 \pm 2.01 \text{ km s}^{-1}$, but the dispersion is larger ($\sigma = 9 \text{ km s}^{-1}$) due to the discordant values measured for five of these stars (see Table 1).

Rotational velocities – To derive the stellar rotational velocities we have used the method described by Lucatello & Gratton (2003). In particular we have computed the Doppler broadening due to the rotation of the object (I_{rot}), which is linked to the rotational velocity ($v_{\text{rot}} \sin i$) by means of a coefficient α : $I_{\text{rot}} = v_{\text{rot}} \sin i / \alpha$ (see equation 3 in Lucatello & Gratton 2003, where I_{rot} is indicated as “ r ”). In principle, the coefficient α should be calibrated by using rotational velocity standards observed with the same instrumental configuration. Although we have not performed such a calibration, the comparison with synthetic spectra computed for different rotational velocities indicates that α is close to unity. We have adopted $1.5 \pm 0.5 \text{ km s}^{-1}$ for the micro-turbulent velocity², and the relation obtained by Gray (1992) for the macro-turbulence. Temperatures have been derived by fitting the wings of the $\text{H}\alpha$ line, which are insensitive to other parameters like metallicity and gravity (Fuhrmann 1993). In particular, we performed a χ^2 minimization between the observed $\text{H}\alpha$ profile and a grid of synthetic spectra computed with different temperatures, by using SYNTHE code (Kurucz 1993). Typical uncertainties for the temperatures are of the order of $\sim 50 \text{ K}$ for

²While this value has been strictly measured for a few SGB stars only, the impact of such an assumption on the derived rotational velocities and chemical abundances is negligible.

the BSSs, and $\sim 100 - 150$ K for the giants. Since the adopted technique is efficient only for rotational velocities up to $\simeq 50 - 60 \text{ km s}^{-1}$, the values of I_{rot} for faster stars have been estimated by comparing the observations in the OI triplet region with rotationally broadened synthetic spectra.

Figure 2 presents the derived rotational index distributions: that of the giants is peaked at $I_{\text{rot}} = 0.0 \text{ km s}^{-1}$, with the highest value being $13.4 \pm 3.4 \text{ km s}^{-1}$ for a SGB. The rotational index distribution for the BSSs (see Table 1) is quite different, with eight stars (40% of the total) being fast rotators, i.e., rotating at more than 50 km s^{-1} (while normal F-G type stars typically spin at less than $\sim 30 \text{ km s}^{-1}$; Cortés et al. 2009). Interestingly, three (out of five) BSSs with anomalous V_{rad} also are fast rotators.

Chemical abundances – As the reference population needed to identify possible anomalies in the BSS surface abundances, we have considered the SGBs, since episodes of mixing and dredge-up may have modified the primordial abundance patterns in the RGBs. Chemical abundances have been derived from the equivalent width measurements by using the WIDTH9 code (Kurucz 1993; Sbordone et al. 2004). Gravities have been determined (within 0.2 dex) by comparing the target position in the CMD with a grid of evolutionary tracks extracted from the *BaSTI Library* (Pietrinferni et al. 2006)³. This also yielded to a mass distribution for the observed BSSs, which peaks at $\sim 1M_{\odot}$, with the most massive object being at $\sim 1.3M_{\odot}$. Abundance errors have been computed by taking into account the uncertainties on the atmospheric parameters and those on the equivalent width measurements. For each star they typically are of the order of 0.1 – 0.2 dex.

The iron content for the SGBs and BSSs has been derived from the equivalent widths of about ten and 2–7 FeI lines, respectively. For the SGBs the resulting average iron abundance is $[\text{Fe}/\text{H}] = -1.10 \pm 0.01$, with a dispersion $\sigma = 0.07$ about the mean, in good agreement with previous values (ranging between -1.20 and -1.07 ; Harris 1996; Ivans et al. 1999; Marino et al. 2008; Carretta et al. 2009). Because of the significant deformation of the spectral line profiles, no iron abundance has been derived for the eight fast rotators. Moreover, technical failures in the spectrograph fiber positioning prevented us to measure it for two additional objects (see Table 1). The iron abundance obtained for the remaining ten BSSs has a mean value of -1.27 and a dispersion $\sigma = 0.10$, consistent, within the errors, with the values derived for the SGBs.

³The derived values for BSSs may be affected by systematic uncertainties, since these stars could be underluminous for their masses (van der Bergh et al. 2001; Sandquist et al. 2003; Mathieu & Geller 2009). While we do not have direct spectroscopic indicators for gravity, uncertainties of 0.2 dex translate in abundances variations smaller than 0.1 dex.

Oxygen and carbon abundances have been computed from the equivalent widths of the OI triplet and the CI lines respectively, and the derived values have then been corrected for non-local thermodynamic equilibrium effects. For O abundances these corrections were derived by interpolating the grid by Gratton et al. (1999); for C abundances we adopted the empirical relation obtained by interpolating the values listed by Tomkin et al. (1992). The resulting average abundances for the SGB sample are $[C/Fe] = -0.16 \pm 0.02$ ($\sigma = 0.17$) and $[O/Fe] = 0.29 \pm 0.02$ ($\sigma = 0.17$). No measurements have been possible for the very fast rotating BSSs and for a few other objects (see Table 1). Hence, we were able to measure both the C and O abundances only for 11 BSSs, out of 20 observed. Figure 3 shows the results obtained in the $[C/Fe]$ – $[O/Fe]$ plane. The values measured for the 11 BSSs are in agreement with those of the SGBs, with no evidence of depletion either in carbon or in oxygen. We finally notice that also in the 3 cases for which only the oxygen *or* the carbon abundance has been measured (see Table 1), the values obtained are in agreement with those of the SGBs.

4. Discussion

Before discussing in details the main findings of the present work it is necessary to verify whether some of the investigated stars do not belong to the cluster. In particular, five BSSs have been found to display anomalous V_{rad} , which may cast some doubts about their membership. However, BSSs #42424 and #64677 have measured proper motions well in agreement with those of the cluster members (Anderson et al. 2006). All the other objects have measured rotational velocities significantly larger than expected for normal stars of the same spectral type, thus making unlikely that they belong to the field. We have also used the Besançon Galactic model (Robin et al. 2003) to derive the radial velocity and metallicity distributions of the Galactic field stars in the direction of M4, within the same magnitude and colour intervals shared by our BSS sample. The V_{rad} distribution is peaked at -14.6 km s^{-1} and has a dispersion $\sigma = 50.7 \text{ km s}^{-1}$. As a consequence, the probability that the BSSs with anomalous radial velocity belong to the field is always smaller than 1.7%. The theoretical metallicity distribution of field stars is peaked at $[Fe/H] = -0.17 \pm 0.02$ ($\sigma = 0.45$). The iron abundance measured in two of the five BSSs with anomalous radial velocity ($[Fe/H] = -1.35$ for #42424, and -1.23 for #64677) clearly is largely inconsistent with the field value and concordant, within the errors, with that of M4 stars. Based on these considerations we therefore conclude that all the BSSs with anomalous V_{rad} are indeed members of M4. We notice that if the discrepancies were caused by the orbital motion in binary systems, under realistic assumptions about the total mass, the orbits would be reasonable for a GC, with separations ranging from a few to 10–20 AU. These BSSs do not show any evidence of photometric variability (Kaluzny et al. 1997), and variations of

V_{rad} with full amplitudes exceeding 3 km s^{-1} on a time interval of 72 hours are excluded by our observations for BSSs #42424 and #64677 (no such information is available for the fast rotators). However, these results do not disprove that they are in binary systems. For instance, they are still consistent with what expected for $\sim 90\%$ of binaries characterized by an eccentricity-period distribution similar to that recently observed by Mathieu & Geller (2009) and populating the tail of the velocity distribution in M4 (Mathieu & Geller, private communication). Indeed, further observations are urged to search for clear-cut signatures of binarity.

The fact that none of the 14 BSSs for which we measured C and/or O abundances shows signatures of depletion is quite intriguing. Out of the 42 BSSs investigated in 47Tuc, F06 found that 6 (14%) are C-depleted, with 3 of them also displaying O-depletion. Accordingly, in M4 we could have expected 1-2 BSSs with depleted carbon abundance, and 0-1 BSS with both C and O depletion. Hence, the resulting non-detection may just be an effect of low statistics and is still consistent with the expectations. Alternatively the lack of chemical anomalies in M4 BSSs might point to a different formation process: while at least 6 BSSs (the CO-depleted ones) in 47Tuc display surface abundances consistent with the MT formation channel, all the (investigated) BSSs in M4 may derive from stellar collisions, for which no chemical anomalies are expected. Finally, it is also possible that the CO-depletion is a transient phenomenon (F06) and (at least part of) the BSSs in M4 are indeed MT-BSSs which already evolved back to normal chemical abundances.

The most intriguing result of this study is the discovery that a large fraction (40%) of the investigated BSSs in M4 are fast rotators, with rotational velocities ranging from $\sim 50 \text{ km s}^{-1}$, up to more than 150 km s^{-1} . We emphasize that this is the largest population of fast rotating BSSs ever found in a cluster. Approximately 30% of the BSSs spinning faster (at $20 - 50 \text{ km s}^{-1}$) than MS stars of the same colour has been recently found in the old open cluster NGC188 (Mathieu & Geller 2009), while BSSs in younger open clusters are found to rotate slower than expected for their spectral type (e.g., Shetrone & Sandquist 2000; Schönberner et al. 2001). For GCs only scarce and sparse data have been collected to date. The most studied case is that of 47Tuc, where 3 (7%) BSSs out of the 45 measured objects (Shara et al. 1997; De Marco et al. 2005; F06) have rotational velocities larger than 50 km s^{-1} , up to $\sim 155 \text{ km s}^{-1}$. The object studied by Shara et al. (1997) is the second brightest BSS in 47Tuc, and all the others are located at the low-luminosity end of the BSS region in the CMD. In addition they span almost the entire range of surface temperatures and distances from the cluster centre. For comparison, apart from being more numerous, the fast rotating BSSs in M4 are also found at all luminosities, temperatures and radial distances (see Figure 4). There is a weak indication that the rapid rotating BSSs in M4 tend to be more centrally segregated than normal BSSs, even if the small number of stars in our sample

prevents a statistically robust result (following a Kolmogorov-Smirnov test, the probability that the two distributions are extracted from the same parent population is $\sim 44\%$). The fastest rotating BSS in M4 (#2000121, with $I_{\text{rot}} \sim 150 - 200 \text{ km s}^{-1}$) corresponds to star V53 of Kalunzy et al. (1997), which is classified as a W UMa contact binary. Interestingly, even in the F06 sample of 47Tuc the fastest BSS (spinning at $\sim 100 \text{ km s}^{-1}$) is a W UMa binary. These two stars also occupies a very similar position in the CMD, at the high-temperature and low-luminosity side of the BSS region.

Unfortunately, from the theoretical point of view, rotational velocities cannot be easily interpreted in terms of BSS formation processes. In fact, fast rotation is expected for MT-BSSs because of angular momentum transfer, but some braking mechanisms may then intervene with efficiencies and time-scales that are still unknown. The predictions about rotational velocity of COL-BSS are controversial (Benz & Hills 1987; Leonard & Livio 1995; Sills et al. 2005). In particular, the latter models show that angular momentum losses through disk locking are able to decrease the BSS rotational velocity from values as high as $\sim 100 \text{ km s}^{-1}$ to 20 km s^{-1} . Hence, the fast rotating BSSs observed in M4 could be generated either through mass transfer activity or through stellar collisions, on condition that no significant braking has (still) occurred.

Three of the BSSs (namely #52702, #53809 and #1000214) of the five with anomalous V_{rad} also are fast rotators. Such a high rotation is difficult to account for by synchronization or mass transfer effects in binary systems, since the orbital separation would not be small enough. A fascinating alternative is that such anomalies in the radial and rotational velocities are due to three- and four-body interactions that occurred in the cluster core: these could have originated fast spinning BSSs and kicked them out to the external regions at high speed (apart from star #1000214, the other two are located well beyond the cluster core radius). Interestingly enough, the dynamical history of the cluster could support such a scenario. In fact, although its stellar density profile is well reproduced by a King model, recent Monte-Carlo simulations (Heggie & Giersz 2008) suggest that M4 could be a post-core collapse cluster, its core being sustained by the “binary burning” activity. The fast rotating and high velocity BSSs could be the signature of such an activity.

While bringing a wealth of information, the results obtained to date for 47Tuc and M4 are still too scarce to provide a clear overall picture. Collecting additional data on rotational velocities and chemical abundances for a significant number of BSSs in a sample of GCs with different structural parameters is indeed a crucial requirement for finally understanding the formation mechanisms of these puzzling stars and their link with the cluster dynamical history.

We acknowledge R. Bedin and Y. Momany for useful discussions, and the referee, Robert D. Mathieu, for helpful suggestions in improving the paper. This research was supported by the Agenzia Spaziale Italiana (under contract ASI-INAF I/016/07/0), by the Istituto Nazionale di Astrofisica (INAF, under contract PRIN-INAF2008) and by the Ministero dell'Istruzione, dell'Università e della Ricerca.

REFERENCES

- Anderson, J., Bedin, L. R., Piotto, G., Yadav, R. S., & Bellini, A. 2006, *A&A*, 454, 1029
- Benz, W., & Hills, J. G. 1987, *ApJ*, 323, 614
- Carretta, E., Bragaglia, A., Gratton, R., D'Orazi, V., & Lucatello, S. 2009, *A&A*, 508, 695
- Cortés, C., Silva, J. R. P., Recio-Blanco, A., Catelan, M., Do Nascimento, J. D., & De Medeiros, J. R. 2009, *ApJ*, 704, 750
- De Marco, O., Shara, M. M., Zurek, D., Ouellette, J. A., Lanz, T., Saffer, R. A., & Sepinsky, J. F. 2005, *ApJ*, 632, 894
- Ferraro, F. R., Fusi Pecci, F., & Bellazzini, M. 1995, *A&A*, 294, 80
- Ferraro, F. R., et al. 2006, *ApJ*, 647, L53 (F06)
- Ferraro, F. R., & Lanzoni, B. 2009, *Revista Mexicana de Astronomia y Astrofisica Conference Series*, 37, 62
- Ferraro, F. R., et al. 2009, *Nature*, 462, 1028
- Fuhrmann, K., Axer, M., & Gehren, T. 1993, *A&A*, 271, 451
- Fusi Pecci, F., Ferraro, F. R., Corsi, C. E., Cacciari, C., & Buonanno, R. 1992, *AJ*, 104, 1831
- Gratton, R. G., Carretta, E., Eriksson, K., & Gustafsson, B. 1999, *A&A*, 350, 955
- Gray, D. F. 1992, *The observation and analysis of stellar spectra*, Cambridge Astrophys. Srv.
- Harris, W. E. 1996, *AJ*, 112, 1487
- Heggie, D. C., & Giersz, M. 2008, *MNRAS*, 389, 1858
- Hills, J. G., & Day, C. A. 1976, *Astrophys. Lett.*, 17, 87

- Ivans, I. I., Sneden, C., Kraft, R. P., Suntzeff, N. B., Smith, V. V., Langer, G. E., & Fulbright, J. P. 1999, *AJ*, 118, 1273
- Kaluzny, J., Thompson, I. B., & Krzeminski, W. 1997, *AJ*, 113, 2219
- Kurucz, R. L. 1993, CD-ROM 13, 18 <http://kurucz.harvard.edu>
- Lane, R. R., et al. 2010, arXiv:1004.4696
- Leonard, P. J. T., & Livio, M. 1995, *ApJ*, 447, L121
- Lombardi, J. C. Jr., Rasio, F. A., & Shapiro, S. L. 1995, *ApJ*, 445, L117
- Lucatello, S., & Gratton, R. G. 2003, *A&A*, 406, 691
- Marino, A. F., Villanova, S., Piotto, G., Milone, A. P., Momany, Y., Bedin, L. R., & Medling, A. M. 2008, *A&A*, 490, 625
- Mathieu, R. D., & Geller, A. M. 2009, *Nature*, 462, 1032
- McCrea, W. H. 1964, *MNRAS*, 128, 147
- Osterbrock, D. E., Fulbright, J. P., Martel, A. R., Keane, M. J., Trager, S. C., & Basri, G. 1996, *PASP*, 108, 277
- Pasquini, L., et al. 2002, *The Messenger*, 110, 1
- Peterson, R. C., Rees, R. F., & Cudworth, K. M. 1995, *ApJ*, 443, 124
- Pietrinferni, A., Cassisi, S., Salaris, M., & Castelli, F. 2006, *ApJ*, 642, 797
- Robin, A. C., Reylé, C., Derrière, S., & Picaud, S. 2003, *A&A*, 409, 523
- Sandquist, E. L., Latham, D. W., Shetrone, M. D., & Milone, A. A. E. 2003, *AJ*, 125, 810
- Sarna, M. J., & de Greve, J.-P. 1996, *QJRAS*, 37, 11
- Sbordone, L., Bonifacio, P., Castelli, F., & Kurucz, R. L. 2004, *Memorie della Societa Astronomica Italiana Supplement*, 5, 93
- Shara, M. M., Saffer, R. A., & Livio, M. 1997, *ApJ*, 489, L59
- Shetrone, M. D., & Sandquist, E. L. 2000, *AJ*, 120, 1913
- Schönberner, D., Andrievsky, S. M., & Drilling, J. S. 2001, *A&A*, 366, 490

Sills, A., Adams, T., & Davies, M. B. 2005, MNRAS, 358, 716

Sommariva, V., Piotto, G., Rejkuba, M., Bedin, L. R., Heggie, D. C., Mathieu, R. D., & Villanova, S. 2009, A&A, 493, 947

Tomkin, J., Lemke, M., Lambert, D. L., & Sneden, C. 1992, AJ, 104, 1568

Tonry, J., & Davis, M. 1979, AJ, 84, 1511

van den Berg, M., Orosz, J., Verbunt, F., & Stassun, K. 2001, A&A, 375, 375

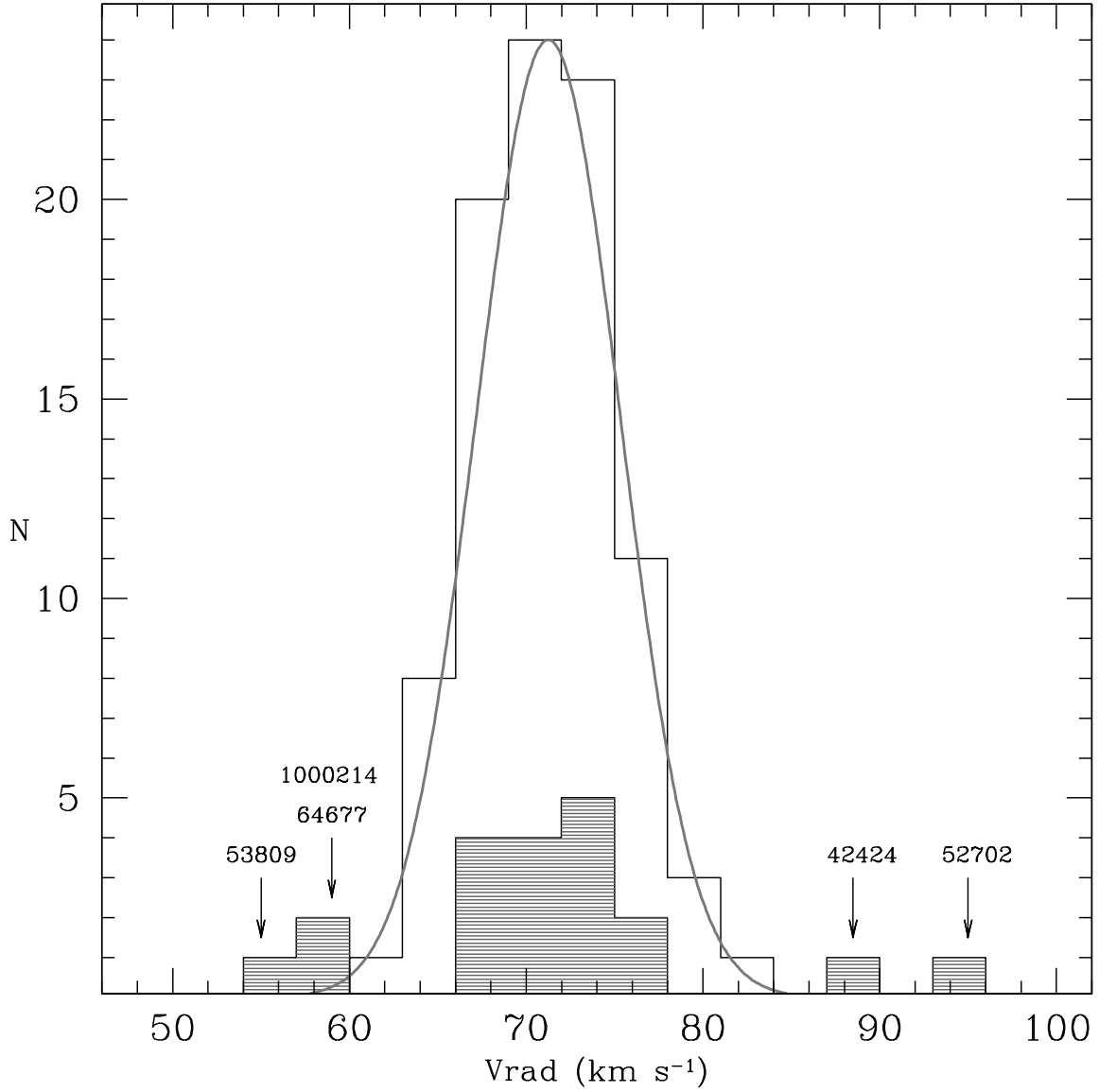


Fig. 1.— Radial velocity distribution for the observed stars in M4. The empty histogram refers to SGBs and RGBs, the shaded histogram to BSSs. The solid curve is the gaussian best-fit to the giant V_{rad} distribution. BSSs displaying discordant radial velocities with respect to the cluster distribution are labelled.

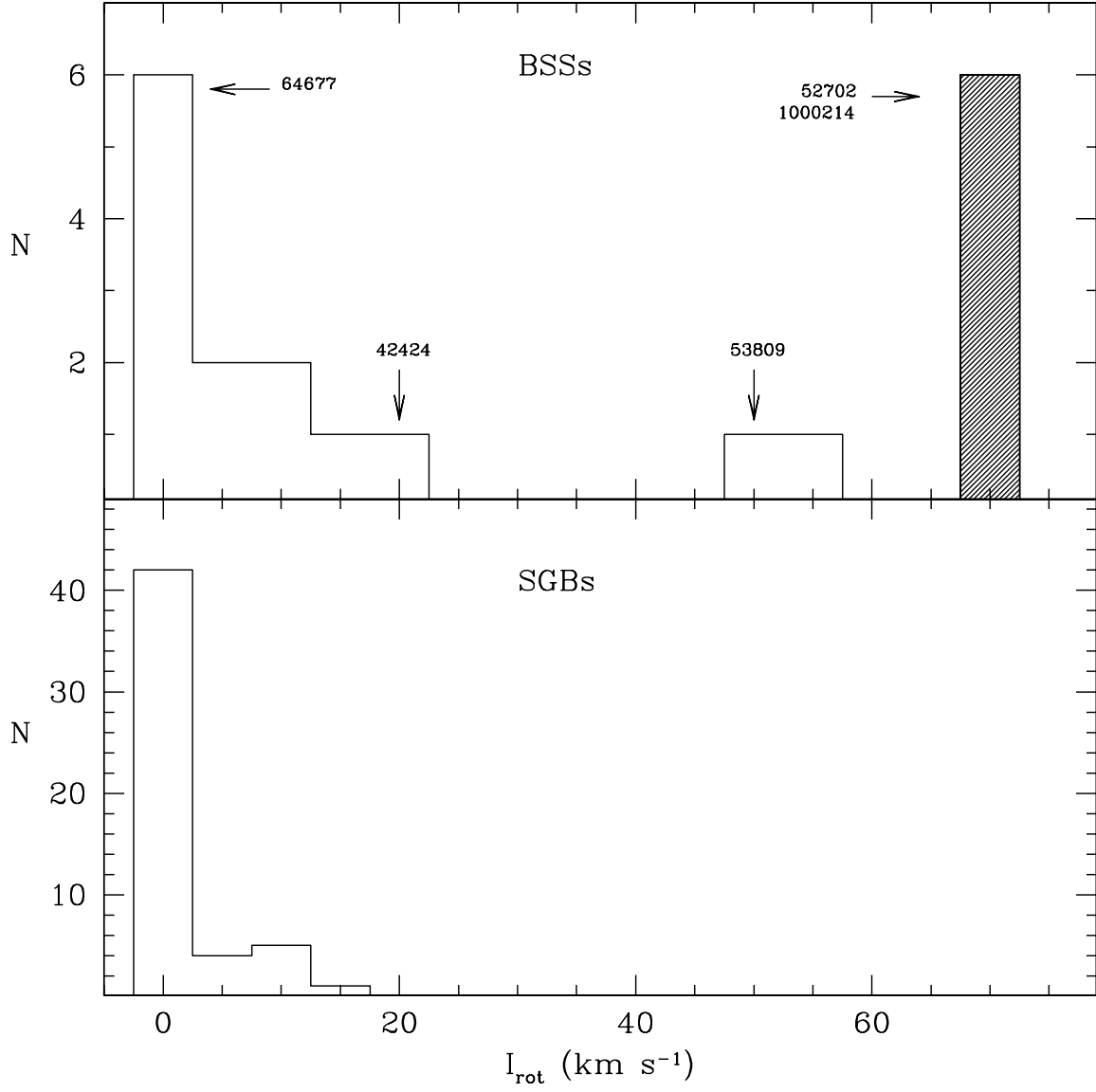


Fig. 2.— Rotational index distribution derived for the observed BSSs (upper panel) and SGB stars (lower panel). The six BSSs with $I_{\text{rot}} \geq 70 \text{ km s}^{-1}$ are all plotted within shaded block. The five BSSs with anomalous V_{rad} are labelled. All RGBs have $I_{\text{rot}} = 0 \text{ km s}^{-1}$ (Mucciarelli et al. 2010, ApJ submitted) and are not shown for clarity.

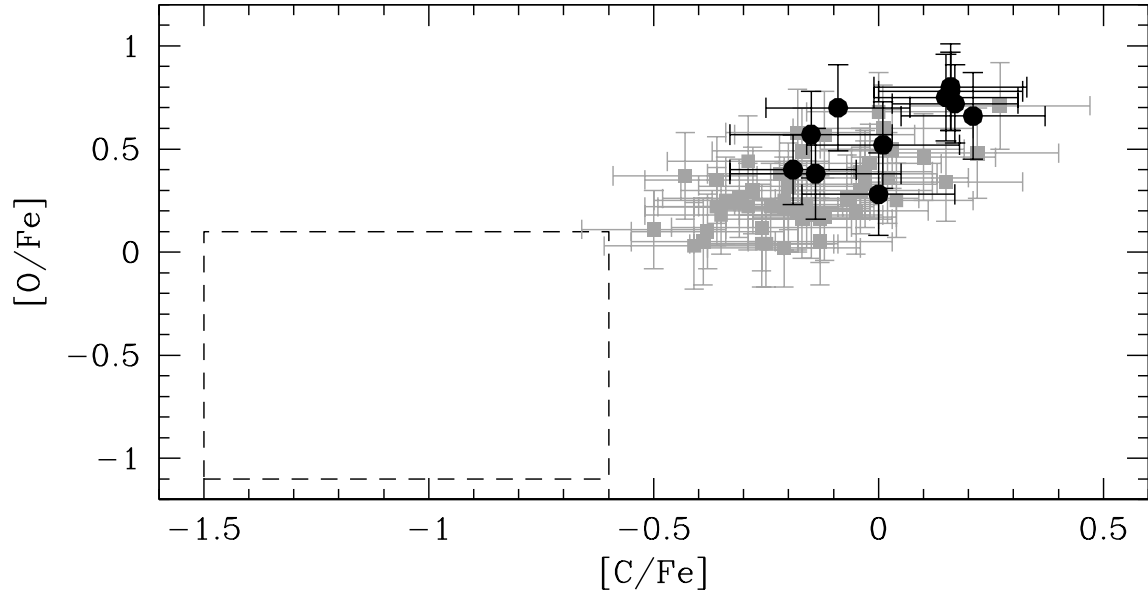


Fig. 3.— $[O/Fe]$ ratio as a function of $[C/Fe]$ for the measured BSSs (black dots) and SGBs (gray dots). The dashed box marks the position of the CO-depleted BSSs observed in 47Tuc (Ferraro et al. 2006).

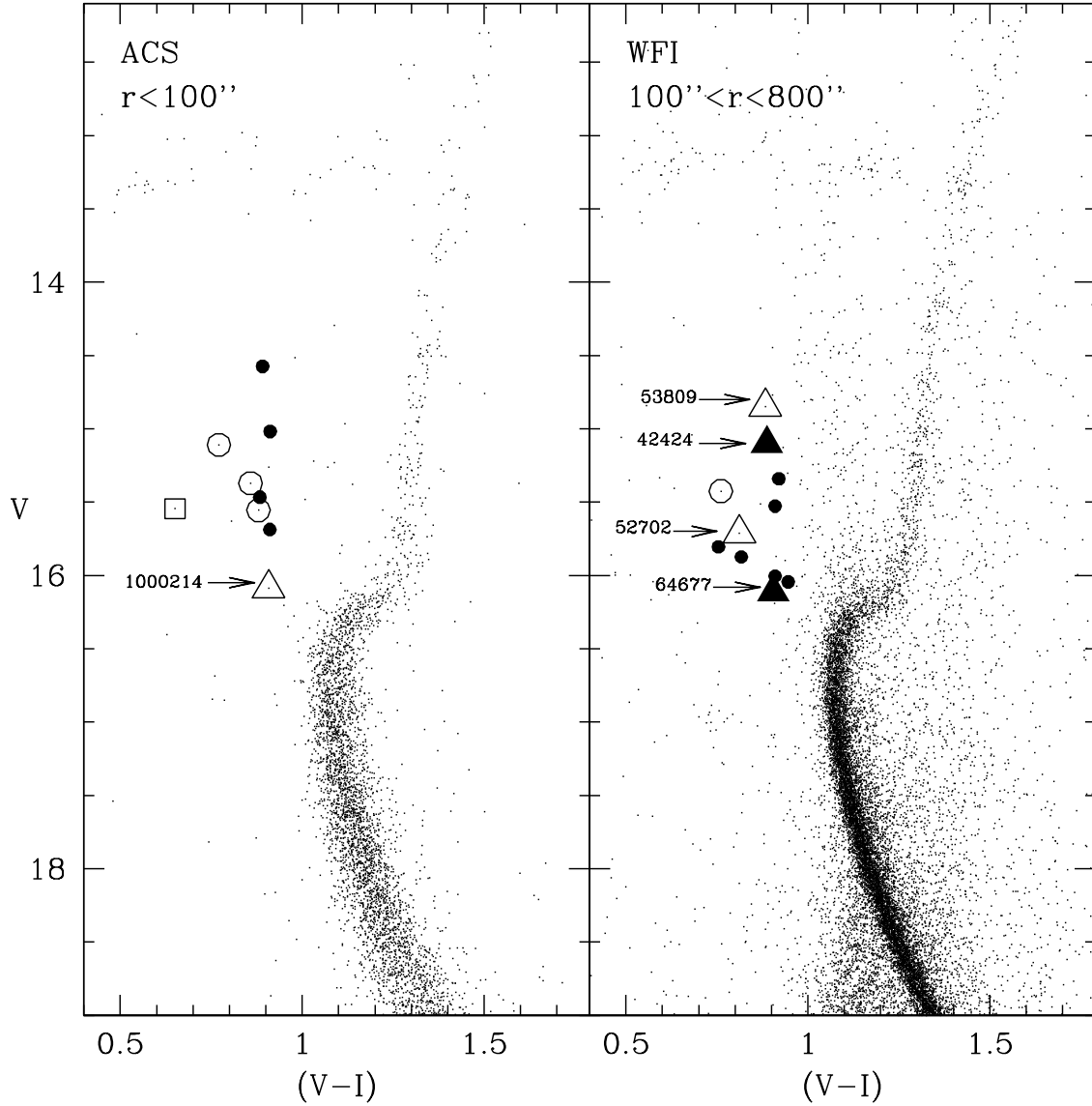


Fig. 4.— CMD of M4 for the ACS and the WFI datasets. The observed BSSs are highlighted: large black dots mark normal BSSs, triangles mark BSSs with anomalous V_{rad} , the square indicates the W Uma star, open symbols mark fast rotators ($I_{\text{rot}} > 50 \text{ km s}^{-1}$).

Table 1. Identification numbers, temperatures, gravities, radial velocities, rotational indices, [O/Fe], [C/Fe] and [Fe/H] abundance ratios for the observed BSSs. “RVa” and “FR” flag the stars with anomalous radial velocities and high rotational speed ($I_{\text{rot}} > 50 \text{ km s}^{-1}$), respectively.

id	T (K)	$\log(g)$	V_{rad} (km s^{-1})	I_{rot} (km s^{-1})	[O/Fe]	[C/Fe]	[Fe/H]	Notes
31209	7300	4.3	74.6 ± 0.6	0.0 ± 2.0	0.70	-0.09	-1.18	
37960	6650	4.0	72.4 ± 0.6	2.0 ± 1.3	0.52	0.01	-1.19	
42424	6850	3.8	87.8 ± 0.9	22.3 ± 0.2	0.80	0.16	-1.35	RVa
43765	6950	4.1	66.3 ± 6.9	56.8 ± 0.1	0.78	0.16	–	FR
44123	6900	4.2	71.2 ± 4.6	10.3 ± 0.4	–	0.10	–	
47856	6450	4.1	66.1 ± 0.6	0.0 ± 2.5	0.57	-0.15	-1.20	
47875	6550	3.9	71.3 ± 0.5	0.0 ± 7.8	0.73	–	-1.37	
52702	6900	4.2	95.1 ± 7.8	70 - 120	–	–	–	FR; RVa
53809	6700	3.8	55.9 ± 6.9	51.6 ± 0.1	0.75	0.15	–	FR; RVa
54714	6500	4.1	74.5 ± 0.6	0.0 ± 6.4	0.28	0.00	-1.20	
64677	6500	4.2	58.6 ± 0.6	0.0 ± 2.0	0.38	-0.14	-1.23	RVa
1000070	6550	3.7	67.4 ± 0.4	4.3 ± 0.7	0.72	0.17	-1.23	
1000117	6700	4.0	72.2 ± 4.6	70 - 100	–	–	–	FR
1000125	7100	4.0	69.5 ± 6.9	80 - 130	–	–	–	FR
1000143	6650	4.0	68.4 ± 0.3	3.2 ± 0.9	0.40	-0.19	-1.29	
1000214	6800	4.2	59.5 ± 5.9	70 - 100	–	–	–	FR; RVa
2000075	6700	3.8	74.5 ± 0.5	8.3 ± 0.4	0.66	0.21	-1.45	
2000085	7100	4.0	70.4 ± 7.8	80 - 120	–	–	–	FR
2000106	6750	4.0	76.1 ± 2.3	12.6 ± 0.3	–	0.10	–	
2000121	7350	4.3	76.4 ± 8.2	150 - 200	–	–	–	FR; WUMa